Supporting Information

Figure S1. Alignment tensors fit to TIMP-1 (light gray above; chain B of PDB coordinates 1uea) and to MMP-3(ΔC) (dark gray below; chain A of 1uea) from their complex. SVD fits and display were performed with Module (*25*) using 96 $^{1}D_{NH}$ RDCs of N-TIMP-1 and 18 $^{1}D_{NH}$ + 7 $^{1}D_{C\alpha H}$ RDCs of MMP-3(ΔC), respectively. Uncertainty in the orientation of the alignment tensors of N-TIMP-1 and MMP-3(ΔC) is simulated by the cluster of dots beyond the tip of each axis. The dots represent the slight variations in alignment tensor from 300 Monte Carlo simulations in which Gaussian noise is introduced to the RDCs to represent the 1 Hz measurement uncertainty. The two clusters of alignment tensors have standard deviations of ± 1.0º for the Euler angle α to A_{Z1} of MMP-3(ΔC) and ± 0.8º for the Euler angle α to A_{Z2} of N-TIMP-1. The N-terminus and α-helices 1 and 2 of TIMP-1 are in the foreground.

Figure S2. Comparison of amide line broadening by Gd-EDTA with depth of amide below surface. A**)** Difference between heights of backbone amide peaks of N-TIMP-1-inhibited MMP-3(ΔC) in the presence of 2 mM Gd-EDTA, $(I_{Gd}/I_0)_{bound}$, and peak heights of the uninhibited MMP-3(ΔC) in the presence of 3 mM Gd-EDTA, $(I_{Gd}/I_0)_{free}$. The peak heights were normalized by the heights, I_0, in HSQC spectra collected prior to addition of Gd-EDTA. For residues (including prolines) lacking an amide assignment for either free or N-TIMP-1-bound MMP-3(ΔC) and for overlapping peaks, no results are plotted. B) Differences in amide proton depth below the Gd-EDTA-accessible surface, r'-r, between the complex and free forms of MMP-3(ΔC), measured from coordinates 1uea and 1sln. To account for the decrease of line broadening with depth, differences in the depths of amide groups below the surface of the two X-ray models were scaled by the square of the shorter depth, improving the correlation with panel (A). Minor discrepancies for residue 188-192 and 224-231 may result from the 1sln model not truly being a free state, in that the small inhibitor affecting the conformation of these segments was removed to model the free state.

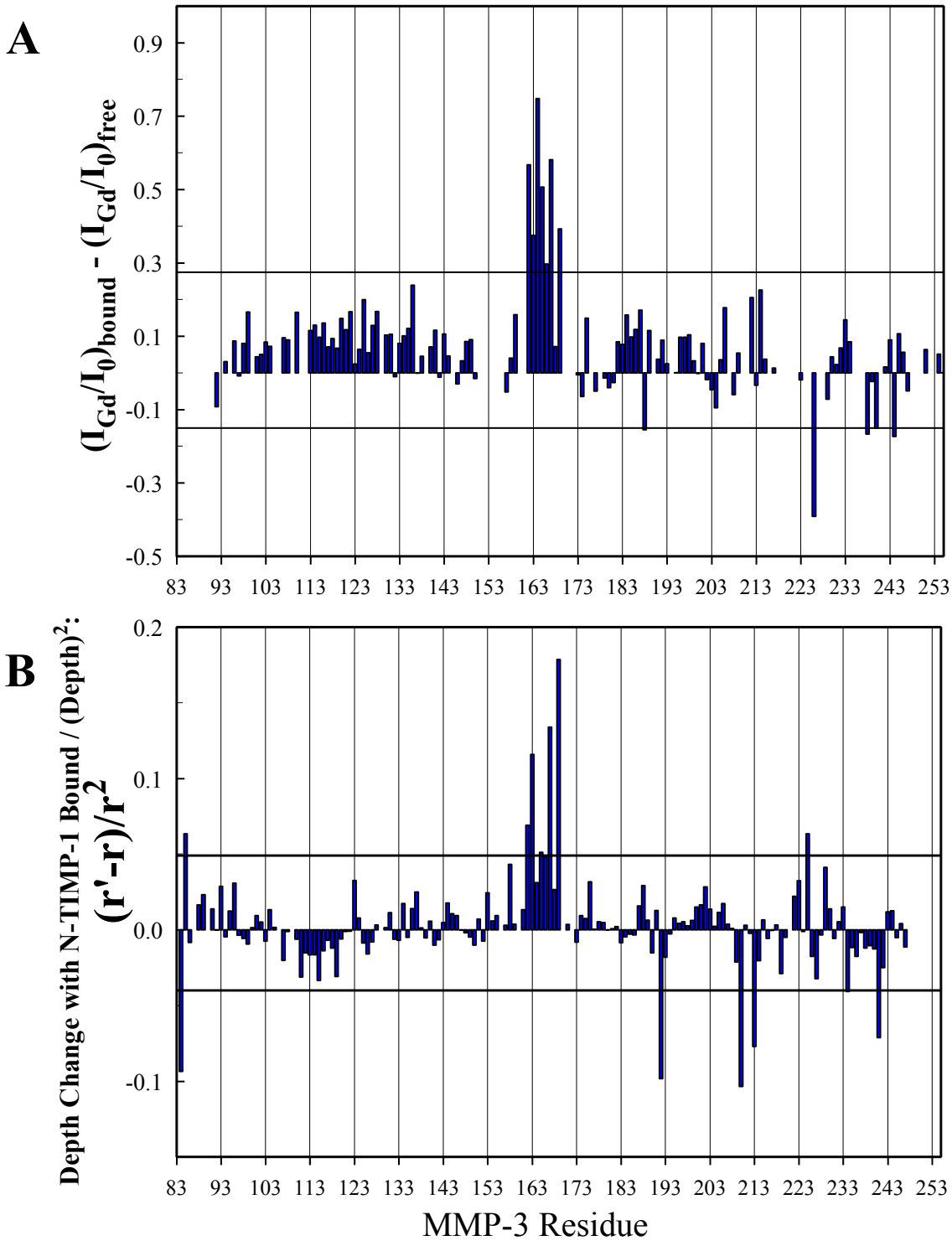
A
$(I_{Gd}/I_0)_{bound} - (I_{Gd}/I_0)_{free}$
0.9
0.7
0.5
0.3
0.1
-0.1
-0.3
-0.5
83 93 103 113 123 133 143 153 163 173 183 193 203 213 223 233 243 253
B
Depth Change with N-TIMP-1 Bound / (Depth)^2:
$(r'-r)/r^2$
0.2
0.1
0.0
-0.1
83 93 103 113 123 133 143 153 163 173 183 193 203 213 223 233 243 253
MMP-3 Residue

Figure S3. The ensemble of 25 (out of 25 calculated) models with N-TIMP-1 (backbone in blue) reoriented in the MMP-3(ΔC) active site have MMP-3(ΔC) coordinates superimposed (ribbon plot). The N-TIMP-1 and MMP-3(ΔC) chains from PDB coordinates 1uea were reoriented using 102 RDCs and 46 intermolecular NOEs using XPLOR-NIH. Of the four outlying models with N-TIMP-1 displaced slightly downward, three have one NOE violated by > 0.5 Å and all four have energies from the simulation that are about 1.5% higher than the lowest energy structure deposited under PDB code 1oo9. In the stereo pair, MMP-3(ΔC) is represented with β-strands as cyan ribbons, helices as red and yellow ribbons, zinc ions as pink spheres and calcium ions as blue spheres.